Case Studies on Transport Policy 13 (2023) 101023

Contents lists available at ScienceDirect

Case Studies on Transport Policy

journal homepage: www.elsevier.com/locate/cstp

Monitoring vehicles with permits and that are illegally overweight on bridges using Weigh-In-Motion (WIM) devices: A case study from Brescia

Roberto Ventura [a], Benedetto Barabino [a,*], David Vetturi [b], Giulio Maternini [a]

[a] Department of Civil, Environmental, Architectural Engineering and Mathematics (DICATAM), University of Brescia, Via Branze 43, 25123 Brescia, Italy
[b] Department of Mechanical and Industrial Engineering (DIMI), University of Brescia, Via Branze 38, Brescia 25123, Italy

ARTICLE INFO

Keywords:
Weigh-In-Motion
Bridge management
Exceptional vehicles

ABSTRACT

Bridges are amongst the most vulnerable elements of road networks. Since vehicles with permits and that are illegally overweight can pose a threat to bridge safety, implementation of monitoring systems for these vehicles has become mandatory. Weigh-In-Motion (WIM) systems are an efficient weight-enforcement solution because they collect data on vehicular mass and other parameters in real time. However, installation and maintenance costs frequently hinder a widespread operational use of WIM systems. Thus, while WIM devices are widespread in America and Asia, they have not yet been applied broadly in Europe. Additionally, the relationships among Gross Vehicle Mass (GVM) and other vehicular characteristics have only been investigated in a fragmentary manner. This real-world case study adopted a data set of 14,800+ overweight vehicles in heavily industrialised northern Italy based on two-months of raw data from WIM devices to: (i) investigate the probability density function on the main characteristics of overweight vehicles, and (ii) to provide Road Authorities (RAs) with a Multiple Linear Regression (MLR) model to predict overweight vehicles' GVM in a more cost-effective way than placing WIM systems on each road segment with bridges. Probability density functions revealed the existence of different vehicle typologies, including lorries with permits and that are illegally overweight, whereas inferential analysis showed MLR's high performance in predicting vehicles' GVM. Minimum axle distance and total axle number were factors that had greater positive effects on the predicted GVM respectively. Conversely, by increasing vehicles' width and length, a reduction in GVM was predicted. These findings could help support practitioners, RAs, and governments to implement rational and less resource consuming administration policies for their bridge assets.

1. Introduction

Road transportation currently dominates inland freight movement by accounting for 77.4% of its total amount (Eurostat, 2022). Hence, a secure and resilient road network is required for the effective operation of inland transportation flows. Therefore, bridges must be considered with a certain priority: they are amongst the most susceptible components of road networks, because they may be subject to structural problems that can make them unserviceable or, in a worst-case scenario, result in a collapse (Zanini et al., 2017). Loss of bridge operativity affects the whole transportation system, with significant social and economic repercussions (Mitoulis et al., 2021). Indeed, a bridge shutdown is a detrimental occurrence that increases user travel time and prevents goods from reaching their destinations on time (Fiorillo and Ghosn, 2019).

After hydraulic actions, vehicle traffic is the main factor that has been found to undermine bridge safety. Indeed, collisions and overloads were the cause of 15.3% and 12.7% of the 1062 bridge failures that occurred in the United States between 1980 and 2012, respectively (Lee et al., 2013). Actually, a recent review on 4500+ bridge failures that occurred worldwide up to 2016, confirmed that vehicle collisions and overloads are among the top five most frequent causes of bridge collapses (Zhang et al., 2022).**

Focusing on overload hazards investigated in this research, findings have shown that extremely heavy vehicles constitute a real threat for bridge safety. These vehicles frequently overstep bridge load limitations, which have occasionally resulted in bridge collapses both in industrialized countries, e.g., the United States and Europe, and in emerging nations, e.g., China (Zhang et al., 2022). Extremely heavy vehicles can be subdivided into those with permits (PMTs), and illegally overweight

* Corresponding author.
E-mail address: benedetto.barabino@unibs.it (B. Barabino).

https://doi.org/10.1016/j.cstp.2023.101023
Received 4 September 2022; Received in revised form 29 April 2023; Accepted 29 May 2023
Available online 9 June 2023

vehicles (IOVs). PMTs are vehicles whose gross vehicle mass (GVM) legally exceeds the vehicle code limits owing to specific authorisations provided for by Road Authorities (RAs). Conversely, IOVs circulate with no specific authorization. On the one hand, before a PMT authorisation can be issued, the RA assesses negative impacts, and the vehicle's weight will be capped according to the conditions of the bridges that are to be traversed. On the other hand, the impacts of IOVs remain unchecked, and the weight of those vehicles is potentially unconstrained (Fiorillo and Ghosn, 2018). Moreover, PMTs are expressly conceived to transport extremely heavy loads, whilst IOVs are usually ordinary vehicles not designed for carrying such large masses.

Therefore, the implementation of monitoring systems for these extremely heavy vehicles is becoming essential for the safe management of road infrastructure and bridges, which has also been recognised by the Italian Ministry of Transportation (Ministero delle Infrastrutture e dei Trasporti, 2020). Indeed, structural safety has become a critical issue in Italy, as highlighted by the recent collapse of bridges, which were built in the second half of the last century, and which were designed to withstand lower vehicle loads than those currently flowing on Italian road networks (Ventura et al., 2020).

Weigh-In-Motion (WIM) systems are an effective solution for automatically collecting data on vehicle weight. According to ASTM (2017), a WIM system is defined as a "*collection of sensors and supporting devices that measure the presence of a moving vehicle and the associated dynamic tyre forces at fixed locations over time*". Apart from the entire vehicle mass, a WIM system can estimate tyre loads, speed, axle spacing, vehicle class corresponding to axle arrangement, and other parameters belonging to the vehicle. Moreover, it processes, displays, and stores these data. Thus, through constructive use of WIM data, institutions could prevent structural damage and implement weight enforcement policies by measuring the GVM acting on bridges in a dynamic way. In this regard, the potential, limitations, cost-effectiveness, and data usage of these devices were reviewed recently (Sujon and Dai, 2021). Findings indicated that on the one hand, the primary advantage of WIM systems is their ability to record such data in real time for all the passing traffic, eliminating the need for human operators to choose random samples of vehicles and to perform manual weighing. Hence, the estimation of the GVM acting on road bridges is a straightforward task provided that WIM data are available for each road segment with bridges. On the other hand, installation and maintenance costs appear to be the biggest obstacles to the widespread operational use of WIM systems in the field. Indeed, many RAs cannot collect WIM data for each road segment with bridges due to the large costs of such systems. Hence, they are not able to measure the GVM of the vehicles passing on road bridges wherever they may be needed and, therefore, to implement rational administration policies for their bridge assets.

Nevertheless, because the GVM also depends on other vehicular characteristics, the development of prediction models for the GVM may be useful to achieve this target for road bridges where WIM measurements are not available. These models can be employed as a part of a less expensive monitoring system (e.g., traffic cameras equipped with image processing algorithms) to recognize vehicles with heavy loads, especially for bridges along secondary routes, where WIM investment costs may not be sustainable. Moreover, these models would enable RAs to plan bridge management actions by individuating the structures more frequently travelled by extremely loaded vehicles.

Whilst WIM devices have been widely employed in the United States and in the Popular Republic of China for several years now, as far as the authors are aware, in Europe, only a few experiences with these devices in the field have been described. Principally, Ventura et al. (2023) provided an initial overview of the flows of overweight vehicles in Italy by applying some descriptive statistics (i.e., cluster analysis) to a WIM dataset. Moreover, the relationship between GVM and other vehicular characteristics has only been investigated in a fragmentary manner in previous studies. As far as the authors know, although sporadic studies in which the relationship between GVM and other vehicular parameters was examined, one parameter at a time, comprehensive research aimed at developing a model to predict GVM as a function of a wide range of other features has never been undertaken.

Hence, by processing real-world raw WIM data on an Italian case-study bridge, this paper aims to contribute to both theory and practice.

From theorical prospective, 1) the probability density functions on the main characteristics of overweight vehicles in a heavy industrialized Italian context are investigated and refined, 2) the relationship between the gross vehicle mass (GVM) and other vehicular features is explored in comprehensive manner, and 3) key factors to predict the GVM of overweight vehicles are identified.

On the practical side, a Multiple Linear Regression (MLR) model is specified, calibrated, and validated to provide RAs with a straightforward (and cost-effective) tool to a preliminary estimation of the GVM of overweight vehicles on road bridges without the need of installing expensive WIM systems on each road portion.

Findings of this paper show that the probability distributions of several vehicular parameters have had a multimodal structure and highlight the existence of various subsets comprising different vehicle typologies, including PMTs and IOVs. Moreover, the proposed MLR model showed high performance in predicting overweight vehicles' GVM, whilst all the parameters included in the best-fit model proved to be highly significant.

The remainder of the paper is organised as follows. Section 2 presents a review of the literature related to WIM applications, Section 3 describes the real-world research context and presents materials and methods used to process raw WIM data, compute probability density functions, and build an MLR model. Then, Section 4 illustrates and discusses the results, whilst finally, Section 5 provides some conclusions and future perspectives.

2. Literature review

Several applications of WIM devices have been described in the literature. Rather than tracing its background, it was deemed most appropriate to summarise the most recent studies up to the year 2022, as can be found in Table 1, whose main points are briefly discussed.

First, the most predominant geographical areas where WIM devices have been applied are in America and Asia, whilst a handful of research describe application of a WIM device in a European context (e.g., Rys and Burnos, 2021; Micu et al., 2019).

Second, while some authors have examined small traffic samples acquired during short monitoring periods at very few WIM sites, others have acquired and processed data on millions of vehicles recorded during multiple years by dozens of WIM stations. Sometimes, WIM data were fused with other data from supplemental sources. For example, Micu et al. (2019) employed a WIM database with free-flowing traffic data to determine a statistical correlation between vehicle lengths and their weights. This correlation was then applied to infer weights in congested traffic conditions from the vehicle lengths recorded by closed-circuit television cameras placed on a bridge.

Third, according to the focus of our analysis, we found that the papers reviewed could be divided into five groups: the Bridge Load (BL) group, the Overweight (OV) group, the Pavement (PV) group, the Structural Monitoring (SM) group, and finally, the Traffic Analysis (TA) group, which are described briefly below, together with some notable additional contributions that are highlighted.

The Bridge Load (BL) group included studies that were mainly aimed at the determination of new load models based on field experimental records, which were collated to consider, for example, the spatial–temporal distribution of vehicle loads, the changes in traffic environments, and hostile actions generated by maintenance works (Huang et al. 2022; Hou et al., 2020; Iatsko and Nowak, 2021; Kim and Song, 2021; Zhou et al., 2021; Yang et al., 2021; Li et al., 2020; Micu et al., 2019). For instance, Li et al. (2020) processed WIM data that had been collected on a long span bridge to detect the vehicle traffic composition,

Table 1
Recent literature (up to 2022) related to the applications of the data acquired by WIM devices.

Authors	Year	Geographical origin of data	Number of WIM sites	Sample size	Period covered	Additional data sources	Clust.	Objective/Relevant insights	Analysis tools
Huang et al.	2022	China	1	Appr. 1 M vehicles	One month	NA	BL	Developing a traffic flow simulation for determining the spatio-temporal distribution of vehicular load on a bridge deck, by considering correlation factors among vehicle parameters.	Descriptive statistics (Copula functions, CDF functions), K-means clustering, Markov chain, Monte Carlo simulation
Iatsko and Nowak	2021	USA	44	Appr. 200 M vehicles	Varying among the sites (from 134 to 365 days)	NA	BL	Updating the statistical parameters of AASHTO bridge's live loads based on WIM data	Descriptive statistics (Normal Probability Plots), Influence line method, Upper Tail Linear Extrapolation method
Kim and Song	2021	South Korea	np	NA	NA	NA	BL	Updating the parameters of a previously developed bridge traffic loads probabilistic model using WIM data	Micro-simulation model, Bayesian Inference method
Hou et al.	2021	Shangai, China	1	Appr. 2 M vehicles	One year	NA	BL	Modelling the vehicle load acting on a long-span bridge using site specific data	Descriptive statistics (finding best distributions using K-S test), Binomial Process, Peaks Over Threshold model
Yang et al.	2021	Shaanxi, China	1	10,000 vehicles	NA	TC	BL	Generating a fine-grained traffic load spectrum using a data fusion method	Data fusion algorithm
Zhou et al	2021	Zhejiang Province, China	1	Appr. 4 M vehicles	300 days	NA	BL	Investigating the impact of maintenance work on the traffic load effects and structural safety of bridges	Traffic microsimulation (SIMBA software, Monte Carlo method), Influence Line method, Extrapolation method (GEV theory based on Gumbel distribution)
Li et al.	2020	Wuhan, China	1	Appr. 0.59 M (minibus + trucks)	One month	NA	BL	Developing a load model for an urban highway bridge using WIM data and considering fatigue damage	Descriptive statistics (Gaussian Mixture Model fitted with Expectation Maximization algorithm), Generalized Extreme Value distribution, FEM, Miner fatigue model
Micu et al.	2019	Scotland, UK	1	Appr. 20 M vehicles	One year (WIM) and five months (cameras)	TC	BL	Evaluating traffic load effect on a bridge using vehicle lengths obtained from images	Image analysis techniques, Descriptive statistics (correlation analysis, PDF estimation using univariate Kernel Density Estimator), Traffic simulation, Influence line method, Extrapolation method (GEV theory based on Gumbel distribution)
Micu et al.	2018	Tennesee, USA	1	Approximately 5.8 M vehicles	One year	NA	BL	Proposing an algorithm which uses image analysis for inferring extreme traffic load from only vehicle lengths.	Bivariate kernel density estimator, Monte Carlo simulation
Bosso et al.	2020	Brazil	1	Appr. 515,000 trucks	5 months	NA	OV	Identifying overloaded truck weight and travel patterns using WIM data to optimize the efficiency of the enforcement activities	Regression Trees
Fiorillo and Ghosn	2018	New York State, USA	21	Appr. 42 M trucks	One year at 18 locations and ten years 3 locations	NA	OV	Proposing an approach for the fragility analysis of bridges subjected to overweight traffic load	Descriptive statistic (Pareto Tail Method), Extrapolation methods (Type I Gumbel and Generalized Pareto distributions), Monte Carlo simulation, nonlinear FEM
Gungor et al.	2018	USA	22	NA	NA	NBI	OV	Computing an overweight fee basing on an economic assessment of overweight vehicle loading on bridges	Descriptive statics (Frequencies analysis, Gaussian Mixture Model), Support Vector Machine
Liu et al.	2018	China	1	Appr. 28,000 trucks	1 month	NA	OV	Proposing a new model for estimating extreme values of vehicle loads on bridges basing on WIM data	Extreme value distribution model (Peak Over Threshold method, Extended Burr XII distribution, K-S test), Markov Chain Monte Carlo simulation
Lu et al.	2018	China	1	Appr. 1.56 M trucks	Two years	NA	OV	Extrapolating the probabilistic extreme effects on long-span bridges under site-specific traffic loads	Descriptive statistics, Rice's Level Crossing Theory, Stochastic Traffic Flow Simulation, FEM
Rys and Burnos	2021	Poland	1	Appr. 251,000 trucks	Two months	NA	PV	Developing a new methodology of heavy traffic axle load spectra (ALS) correction due to weighing errors (systematic and random) that occur in WIM systems.	Descriptive statistics (probability distributions, load spectrums)
Zhao et al.	2021	New Jersey, USA	87	NA	NA	NA	PV	Analysing the impact of traffic loading on pavement performance.	Nonlinear Regression model, Support Vector Regression

A = Accelerometers; AVC = Automatic Vehicle Classifier; BL = Papers focused on bridge load analysis; DG = Displacement Gauges; FEM = Finite Element Model; GPS = Global Positioning System; L = Lidar; NA = Not Available; NBI = National Bridge Inventory; OV = Papers focused on overweight vehicles analysis; PV = Papers focused on road pavements; SG = Strain Gauges; SM = Papers focused on structural monitoring; T = Thermistors; TA = Papers focused on traffic analysis; TC = Traffic Cameras; TTMS = Telemetric Traffic Monitoring Sites.

which was processed to determine probability distributions on gross vehicle weights. Thus, the maximum value of the vehicle loads that were expected to act on the case-study bridge during the design reference period were predicted, whilst at the same time, a fatigue vehicle load model, that took accumulated damage into account, was proposed.

The Overweight (OV) group involved papers that focused primarily on the identification of overweight lorries and the evaluation of the detrimental effects that they produce on the service life of bridges and pavements (Bosso et al., 2020; Fiorillo and Ghosn, 2018; Liu et al., 2018; Lu et al., 2018; Gungor et al., 2018). Notably, using WIM datasets, Bosso et al. (2020) proposed a method to detect overloaded lorry travel patterns and loading characteristics. Results indicated that lorry type was the most important variable that could be used to distinguish legally loaded from overloaded vehicles. Indeed, larger lorry classes showed higher percentages of overweight vehicles than compact and midsized trucks.

In the Pavement (PV) group, WIM data were processed to support the new design of road pavements, as well as to aid the maintenance of existing roadways (Rys and Burnos, 2021; Zhao et al., 2021; Ren et al., 2019; Li et al., 2019). Worthy of note is the research by Ren et al. (2019), which showed that a lower proportion of empty lorries on the road can lessen pavement damage by distributing the total freight among all the vehicles more uniformly whilst lowering the mean payload values.

In the Structural Monitoring (SM) group, WIM devices were integrated with other instruments to conduct real time monitoring of bridges' structural health. These analyses had several goals such as triggering early warning systems to prevent overturning events in single-column box-girder bridges (Dan et al., 2021; Ge et al., 2020), or linking lorry weights with structural responses to detect and predict potential damage (Hou et al., 2020).

In the Traffic Analysis (TA) group, lorry flows were analysed at three different levels: 1) singular road sections, 2) road segments, and 3) overall road networks. Each of these analyses comprised different scopes, such as characterizing vehicle weight distributions, tracking vehicle movements, and investigating state-wide freight tonnage (Peng et al., 2021; Rivera-Royero et al., 2021; Hernandez and Hyun, 2020; Liu et al., 2020; Regehr et al., 2020; Demiroluk et al., 2018; Cetin et al., 2014). By way of illustration, Hernandez and Hyun (2020) estimated gross vehicle weight distributions at traffic count sites (where weight measurements were not available) by fusing weight data from the nearby WIM sites and position data from GPS devices. Good performance was observed when weight distributions were compared to the ground truth. Conversely, Regehr et al. (2020) characterized payload distributions for predominant axle configurations and lorry body types. Their findings showed that the load distributions for lorries with van, flat deck, and container body types included lorries with GVMs over the entire mass range, regardless of axle configuration (i.e., from empty to fully loaded). The variety of goods and commodities that these lorries transport and the typical nature of the services they provide were found to be the causes of this varied loading pattern. Contrarily, lorries with dump, hopper, and tanker body types – which often transport large or bulk materials – tend to either travel fully laden (i.e., close to the GVM limit) or empty.

In addition, whilst some studies have adopted simply descriptive statistics, others have analysed WIM data by applying more complex mathematical tools. Amongst these, an extreme value analysis and a Monte Carlo simulation, based on samples acquired by WIM devices during relatively short monitoring periods, were applied to infer lifetime load actions on bridges, whilst at the same time, the structural response was simulated using Finite Element Models (FEMs). Moreover, though cluster analyses have been employed to group data according to similarities, several predictive models have also been adopted in different contexts, ranging from traditional regressions to more innovative methods based on the Bayesian interpretation of probability or Machine Learning techniques.

Undoubtedly, all these studies have contributed significantly to the analysis of raw WIM data with separate goals. In addition, they have provided valuable insights on vehicle mass distributions and on some overweight vehicle features. However, at least two gaps persist. First, even though there have been several applications of WIM devices in America and Asia, in Europe this research continues to be scarce. For instance, aside from Ventura et al. (2023), who provided a cluster analysis on a wide set of vehicular features to recognize heavy vehicle groups, none have used WIM systems in Italy to examine the flows of overweight lorries. Therefore, given that the patterns of lorry populations have shown strong spatial dependence (Demiroluk et al., 2018), research examining WIM data collected across European countries using straightforward statistical indicators appear to be necessary.

Second, the relationship between gross vehicle mass (GVM) and other features, such as passing DateTime, passing speed, vehicle width, vehicle length, number of axles, axle and interaxle types, has been investigated, at best in a fragmentary manner in previous studies. Actually, only sporadic studies have been undertaken in which the relationship that GVM has with other vehicular parameters has been investigated, with just one parameter at a time. For example, Micu et al. (2018) observed a positive statistical correlation between vehicle lengths and their weights. Hence, they proposed an algorithm that could generate simulated GVM data based on vehicle lengths. Even though the simulated data was found to be globally consistent with the statistical weight distributions that were experimentally observed, the algorithm was not accurate in its singular predictions of the weight of individual vehicles. Subsequently, Regehr et al. (2020) observed a significant relationship between payload distributions and lorry body types, whilst Bosso et al. (2020) confirmed that lorry type can be a useful variable to distinguish among legally loaded and overloaded vehicles. Conversely, as far as the authors know, a comprehensive study aimed at developing a model to predict GVM as a function of a wider set of other features has not yet been included in the literature. Consequently, the aim of this paper is to comprehensively fill in these two gaps in current research.

3. Materials and methods

3.1. Research context

The investigation was conducted in the city of Brescia, which is in the eastern part of the Lombardy Region in Italy. Brescia, which has 196,850 residents, constitutes the region's second largest city whilst over 1.25 million people live in its province (ISTAT, 2022). Brescia is one of Italy's most significant industrial, commercial, and social hubs, and as such, it attracts and originates a large amount of daily vehicle traffic (De Aloe et al., 2023). Notably, numerous businesses that process iron and steel goods and that manufacture heavy and high-density metal products can be found in the Brescia metropolitan area. Furthermore, near the city there are several quarries where stone materials are extracted (e.g., Botticino Marble), which are employed for construction works. Therefore, there is a strong demand for heavy lorry transportation that impinges on the Brescia Road network. However, the advanced age of a relevant portion of the bridge structures along these roadways may not be able to safely meet this demand.

Consequently, to achieve some insight about the heavy transportation demand on Brescia's bridge assets, a structure along Brescia's South Ring Road was chosen as a case study in accord with the local RA, i.e., the Province of Brescia. The South Ring Road, one of the city's arterial roadways, is a part of the main road system, which carries the largest volumes of traffic and the highest share of commercial vehicles (Faccin et al., 2011). The bridge selected is a simple-supported overpass structure that takes the Ring Road over a secondary road. Its span length is approximately 23.50 m, and it comprises 13 longitudinal precast concrete girders and a mid-span transversal cast-in-situ stiffening girder (Fig. 1). At the case-study bridge, the roadway segment has two separate carriageways, with two lanes in each direction. Since heavy vehicle transit is forbidden in the left lane, and due to budget constraints, the

Fig. 1. View of the case study bridge (Source: The authors).

WIM device was installed on only the right lane of the northbound carriageway.

3.2. Methodological framework

To investigate the main characteristics of overweight vehicles and develop a model to predict those overweight vehicles' GVM as a function of a broad set of other features, the following five-step methodology was implemented for this research:

- In Step 1, since traffic load has strong spatial dependence, the site-specific raw data were collected through a WIM system placed near the case-study bridge and stored in a Cloud Database.
- In Step 2, the raw data were downloaded onto a local machine, pre-processed to remove outliers and to exclude the lightest vehicles from the subsequent processing, as the research was focusing on overweight lorries.
- In Step 3, the probabilistic distribution of each vehicular parameter measured by the WIM device was determined, plotted on cartesian graphs, and qualitatively analysed to discover any significant patterns and provide insights on traffic composition.
- In Step 4, GVM values were adjusted to account for dynamic amplification phenomena, since the vehicle-bridge interaction could lead to a "Dynamic" GVM acting on the bridge in a manner that was greater than a static GVM.
- In Step 5, an MLR model was set up to predict the "Dynamic" GVM as a function of a set of explanatory factors that could be simply inferred using instruments that are less expensive than WIM devices, e.g., traffic cameras. Hence, the performance of the model set up and the effect each explanatory factor has on predictions were evaluated.

Some details of these steps are indicated in what follows.

3.2.1. Step 1: Collecting raw data on passing vehicles through WIM

The first step is required to collect vehicle weight data for analysis. Therefore, a WIM device was placed on the northbound approach to the case-study bridge. This device consisted of two stainless steel plates installed on the road surface, fibre optic sensors, and a connection to a data logger. The selection of fibre optic sensors was preferred over other technologies because these sensors can operate under a variety of conditions, such as a wide range of vehicle speeds and adverse weather conditions, without incurring any significant loss of accuracy. Optical fibre-based WIM devices infer the vehicle load when it acts on the plates though phase shift measurements by exploiting photo-elastic properties in glass fibres induced by the vertical compressive forces applied by the passing tyres (Yannis and Antoniou, 2005). The WIM device used was rated as a "10 accuracy class" instrument according to the International Organization of Legal Metrology (OIML) recommendations (OIML, 2006), which means that the device can determine the vehicle mass with an accuracy of $\pm 10\%$. The system was homologated to operate under all weather conditions within a temperature range between -10 °C and 40 °C, which is compatible with the environmental conditions of the case-study site.

Several physical parameters were measured for each passing vehicle as is usual for WIM standard architecture. They include the passing datetime, the gross vehicle mass (GVM), the passing speed, the vehicle length, the vehicle width, the number of axles, the typology of each axle (i.e., single, or double wheel), the mass acting on each axle and the distance between each pair of axles (i.e., interaxle). These parameters were measured in real time and then they were processed by an acquisition unit, streamed through an internet connection to a Cloud Database platform and stored as JSON files, i.e., an open standard format based on the JavaScript programming language that uses human-readable text to store and transmit data objects consisting of attribute–value pairs and arrays (JSON.org, 2002).

3.2.2. Step 2: Downloading, pre-processing, and filtering raw data

Once the JSON files were available from the field, in Step 2, they were downloaded onto a local machine for processing. Next, the JSON files were uploaded into a MATLAB© software environment and parsed with the embedded "jsondecode" algorithm to convert the JSON objects into a structure array that can be more easily handled inside the selected software platform (MathWorks, 2022a; MathWorks, 2022b). Afterwards, as the WIM data were automatically collected, the datasets were pre-processed to remove any outliers, as is standard in other fields (Barabino et al., 2017). These outliers may have been observations in which the WIM did not compute some vehicular parameters or where some of computed parameters were judged not to be sufficiently reliable. There were several motivations for this lack of reliability, for example, tyre passage outside the plate boundaries, excessive vehicle

acceleration or out of range passing speed. The WIM system automatically recognised and labelled these outliers by adopting a proprietary algorithm.

Next, the pre-processed data were filtered by setting a minimum threshold for the GVM parameters that would eliminate the lightest vehicles, since the research was focused on overweight lorries. Specifically, a 44,000 kg threshold was adopted because this weight is the maximum mass limit imposed by the Italian Code for ordinary lorries (Repubblica Italiana, 2015). Indeed, in Italy, the only vehicles that can exceed this mass limit and travel without a case-specific authorization are construction machinery with a weight of up to 54,000 kg. However, these vehicles can only circulate on authorized roads and must pay a specific fee to compensate for the greater damage incurred on public infrastructure.

3.2.3. Step 3: Determining the probabilistic distribution of each vehicular parameter

Once the WIM data were processed as detailed in the previous step, some descriptive statistics were run to investigate the distribution of these data. Specifically, according to Step 3, because vehicular parameters constituted continuous, discrete, or categorical random variables, their Probability Density Functions (PDFs), Probability Mass Functions (PMFs) or Categorical Distributions (CDs) were determined so that their statistical distributions could be examined.

More precisely, let:

- I be the set of observations after pre-processing and filtering procedures, and $i \in I$ be an individual observation.
- X be the generic parameter gathered by WIM and x_i be the value that it assumed on the observation $i \in I$.
- B be the set of frequency bin for a considered continuous variable and $b \in B$ be an individual bin.
- Δb be the amplitude of the frequency bin for a continuous variable.
- D be the set of possible values for a considered discrete variable and $d \in D$ be an individual value.
- C be the set of possible categories for a considered categorical variable and $c \in C$ be an individual category.
- PDF_b be the PDF of a considered continuous random variable, representing the likelihood of an observation to belong to a certain frequency bin $b \in B$.
- PMF_d be the PMF of a considered discrete random variable, representing the probability the observed value is exactly equal to a specific value $d \in D$.
- CD_c be the CD of a considered categorical random variable, representing the probability of an observation to belong to a specific category $c \in C$.

Hence, in that the GVM, speed, width, length, axle mass and axle distance are random continuous variables, their PDFs were computed as follows:

$$PDF_b = \frac{count(x_i \in b)}{|I| \bullet \Delta b} \forall i \in I; \forall b \in B \tag{1}$$

Similarly, since axle number is a random discrete variable, its PMF was determined according to the following equation:

$$PMF_d = \frac{count(x_i = d)}{|I|} \forall i \in I; \forall d \in D \tag{2}$$

Likewise, since axle typology is a random categorical variable, its CD was calculated as follows:

$$CD_C = \frac{count(x_i \in C)}{|I|} \forall i \in I; \forall c \in C \tag{3}$$

Finally, the computed distributions were plotted on cartesian graphs and qualitatively analysed to provide some insights on the measured vehicular parameters and to discover any significant patterns.

3.2.4. Step 4: Adjusting observed GVM to account for dynamic amplification phenomena

It is well known that because of the vibration caused by road surface roughness and the interactions between the vehicles and the bridge, the traffic load causes dynamic effects (Ma et al., 2019). Therefore, the observed values of GVM were adjusted to account for dynamic amplification phenomena, as described in step 4. Actually, static loads that are increased by the "Dynamic Load Factor" (DLF) are traditionally used to design bridges. This is a dimensionless factor, which is a function of the span length or the first flexural natural frequency of the bridge, and which indirectly incorporates the dynamic effects of moving vehicles in the design (Moghimi and Ronagh, 2008).

In this case study, the modelling of a simply supported prismatic beam subjected to a constant force traveling at a constant speed was considered. Although this modelling does not consider parameters such as road roughness, suspension characteristics, or tyre characteristics, it was adopted as a preliminary approach to the problem. Indeed, since many bridges consist of simply supported girders, this model provides a useful insight into their dynamic behaviour.

More formally, let:

- DLF be the Dynamic Load Factor, i.e., the ratio between the maximum dynamic response and the maximum static response of the structure, respectively.
- v $[km/h]$ be the passing speed of the vehicle.
- $\alpha[m/s]$ be an empirical parameter approximately constant with span length and dependent on the structural type. For simply supported structures, the constant value of 60 is indicated for prestressed concrete box girder deck units, while the constant value of 120 is reasonable for prestressed concrete girder bridges and composite concrete slab and steel girder bridges (Chan and O'Connor, 1990).
- $dyn\_GVM[kg]$ be the "Dynamic" GVM, i.e., a fictitious mass, larger than the static mass, which considers that the effects are due to dynamic amplification.

According to Ventura et al. (2020), the DLF associated with each vehicle passing on the bridge was estimated as follows:

$$DLF = \frac{1}{1 - \frac{v}{3.6\frac{m \bullet h}{km \bullet s}} \bullet \frac{1}{2\alpha}} \tag{4}$$

Hence, by assuming that the structural response was proportional to the applied vehicle mass, then the "Dynamic" GVM of each passing vehicle was adjusted by multiplying the static value by the DLF, which is:

$$dyn\_GVM = GVM \bullet DLF \tag{5}$$

3.2.5. Step 5: Fitting an MLR to predict "Dynamic" GVM as a function of the other vehicular parameters

Once the GVM was adjusted to reflect the dynamic amplification phenomena, according to Step 5, an MLR model was fitted to predict the response variable, i.e., *dyn_GVM*, as a function of a set of explanatory factors computed on data acquired by the WIM system for each vehicle passing on the case-study bridge. The list of explanatory factors was selected considering that RAs may also gather these factors using tools that were less expensive than the WIM, such as traffic cameras.

Implementation and comprehension of the MLR model is straightforward since it adopts simple notions of statistics. In fact, the coefficient value – which is the partial derivative of the response variable with respect to the considered explanatory variable – shows the relative "importance" of each factor in explaining the response variable, by maintaining all other variables fixed at their means. For example, a greater coefficient for an explanatory variable indicates a greater dependence of the response variable. Furthermore, the sign of the

parameters is also essential since a negative sign would denote a decrease in the *dyn_GVM* prediction for each increase in the associated explanatory variable, and vice-versa.

More formally, let:

- $\widetilde{dyn\_GVM}_i$ be the predicted Dynamic Gross Vehicle Mass for the observation $i \in I$.
- F be the set of explanatory factors (variables, or predictors), $f \in F$ be an individual factor, and f_i be the value assumed by the factor f in the observation $i \in I$.
- α_0 be the constant of the regression (i.e., hyperplane intercept).
- α_f be the regression coefficient associated to the parameter $f \in F$.

Then, the value of $\widetilde{dyn\_GVM}_i$ was statistically predicted for each $i \in I$ through the MLR model, as follows:

$$\widetilde{dyn\_GVM}_i = \alpha_0 + \sum_{f \in F} \alpha_f f_i \forall i \in I \tag{6}$$

Before running the fitting procedure, let:

- $TR \subset I$ be set of observations adopted for training the MLR.
- $TE \subset I$ be set of observations adopted for test the MLR.

This subdivision is necessary to implement a model validation technique, which relies on unbiased out-of-sample evaluation. The training set was presented to the model during the fitting process, and the coefficients were determined to minimize the prediction error. Conversely, the testing set had no effect on fitting and so provided an independent measure of model performance. The splitting ratio was assumed to be 70% and 30% for training and testing, respectively (Fertlitsch, 2021).

The best possible coefficients of the MLR model were estimated by applying the ordinary least squares method as follows. First, a full MLR was run including all factors. Next, the parsimony principle was contemplated to achieve an enhanced and reduced model comprising only a subset of variables. The backward and forward stepwise regression procedures were adopted to select the best variables to be included in the model by eliminating superfluous explanatory factors. However, being automated processes, these techniques might occasionally fail to exclude some pairs of strongly correlated factors. Consequently, some highly correlated explanatory factors were manually removed by analysing a correlation matrix. A Pearson correlation coefficient with an absolute value greater than 0.8 was assumed as an exclusion rule to prevent multicollinearity (Shrestha, 2020). Basing the selection criteria on the highest adjusted R-squared value (denoted by R^2_{adj}), the F value and its related p-value of the obtained model, the best model was chosen.

After the model was built, the following goodness-of-fit statistics were considered to assess its performance: the R^2_{adj}, and the linear correlation between predictors and the response variable, with the latter indicated by the global F-test and the corresponding significance value. The sign of each coefficient and its significance were also evaluated.

Subsequently, a residuals analysis was performed to assess the validity of the null mean and normal distribution assumptions (i.e., the random disturbance term across all predictors and observations). More formally, let ε_i be the residual of the predicted *dyn_GVM* for the observation $i \in I$:

$$\varepsilon_i = dyn\_GVM_i - \widetilde{dyn}_{GVM\,i} \forall i \in I \tag{7}$$

Hence, the mean of residuals (denoted as $\bar{\varepsilon}$) on the training subset was calculated as follows:

$$\bar{\varepsilon} = \frac{\sum_{i \in TR \subset I} \varepsilon_i}{|TR|} \tag{8}$$

Finally, some Measures of Errors (MoEs) were computed on the training and test subsets to better assess prediction performance. These measures include the Mean Absolute Error (*MAE*), Root Mean Squared Error (*RMSE*), the the Mean Absolute Percentage Error (*MAPE*) and the Coefficient of Variation (*CoV*). They act as indicators of the average magnitude of the residuals in a set of predictions, without considering their direction. Since they are negatively oriented scores, lower values are better. More precisely, as for the training subset (*TR*), MoEs were computed according to the equations from (9) to (12).

$$MAE = \frac{\sum_{i \in TR} |\varepsilon_i|}{|TR|} \tag{9}$$

$$RMSE = \sqrt{\frac{\sum_{i \in TR} \varepsilon_i{}^2}{|TR|}} \tag{10}$$

$$MAPE = \frac{1}{|TR|} \sum_{i \in TR} \left| \frac{\varepsilon_i}{dyn\_GVM_i} \right| \tag{11}$$

$$CoV = \frac{RMSE}{\frac{\left(\sum_{i \in TR} dyn\_GVM_i\right)}{|TR|}} \tag{12}$$

As the for the test subset (*TE*), MoEs were computed according to the same previous equations where $|TR|$ was replaced with $|TE|$.

4. Results and discussion

4.1. Raw WIM data collection, preparation, and pre-processing

According to Step 1, Raw WIM data were collected over a two-month observation period from 1 January 2022 to 28 February 2022. To ensure that environmental temperatures were always within the operational range recommended by the WIM producer, data provided by a weather station near the case-study bridge were examined. The results confirmed that the minimum and maximum values measured daily did not exceed temperature limits (Fig. 2).

During the timeframe considered, raw data of 1,005,782 passing vehicles were recorded by the WIM system. The data were then streamed in real-time through an internet connection to a Cloud Database platform where they were stored as JSON files. Next, at the end of the monitoring period, the JSON files (containing approximately 1.38 GB of raw data) were downloaded onto a local machine according to Step 2. Afterwards, the JSON files were uploaded into a MATLAB© software environment, where they were converted into a structure array. Once outliers were eliminated through a proprietary pre-processing procedure, a total of 665,090 observations were preserved. Finally, a set of 14,861 vehicles (I) with a GVM greater than 44,000 kg were identified by employing a filtering procedure.

4.2. Building the probability density functions

As a result of Step 3, the PDFs, the PMF and the CD associated with continuous, discrete, and categorical vehicular parameters were numerically computed by applying Eqs. (1), (2) and (3), respectively. The cartesian graphs from the computed distributions are in Fig. 3.

Generally speaking, several PDFs displayed a multimodal form. The speed and width distributions were the only parameters that had a monomodal pattern.

Focusing on the PDFs, on the one hand, subsequent considerations emerged. Regarding GVM, the distribution showed a trimodal shape, with a high peak at about 45,000 kg and two noticeably lesser peaks at roughly 56,000 kg and 96,000 kg. The multimodal shape is like that observed in different geographical contexts, such as the Chinese (Li et al., 2020; Lu et al., 2018), the American (Fiorillo and Ghosn, 2018) and the Australian (Ren et al., 2019). The first peak probably

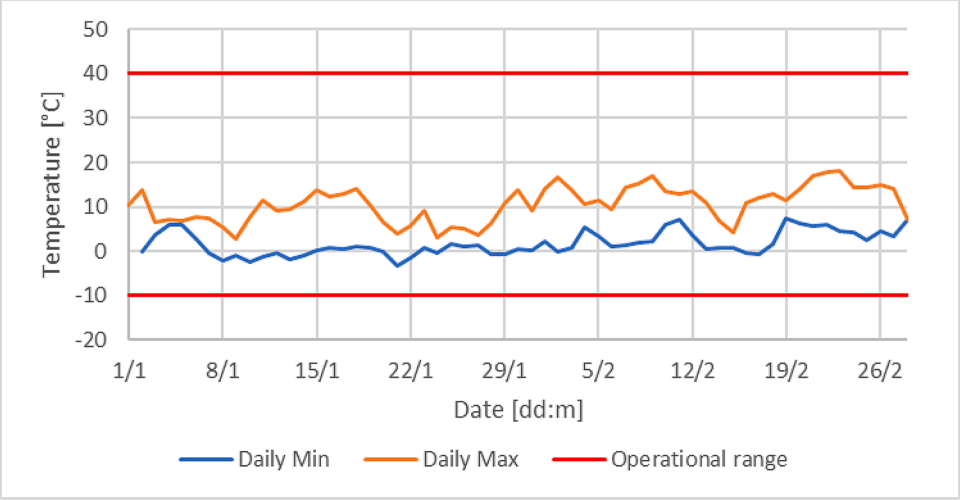

Fig. 2. Environmental temperatures near the case-study bridge during the monitoring period (ARPA Lombardia, 2023). Daily minimums and maximums were always inside the operational range prescribed by the WIM producer.

corresponds to articulated lorries or road trains, which were only slightly overweight, whereas the second peak is probably related to slightly overweight construction machinery, for which the Italian Code allows the GVM threshold to be extended up to 54,000 kg by paying a compensation fee for the greater deterioration incurred by the infrastructure (Italian Republic, 2015). Conversely, it is likely that PMTs are the main component of the third peak, since the observed GVM is well beyond mass limits imposed for ordinary lorries and, thus, an overloading rate of such a magnitude (more than 200%) appears to be unrealistic.

The length parameter PDF also displayed many peaks, with the three highest ones located close to 9 m, 12 m, and 13.5 m. This suggests the existence of different lorry typologies inside the sample. Additionally, the axle mass is bimodal distributed, with the first and the second maximums being close to 8300 kg and 12,500 kg, respectively. Although the observed bimodal shape is consistent with the findings of previous research (Rys and Burnos, 2021), the axle mass values related to the two peaks were higher than expected. Indeed, by focusing on five-axle articulated lorries passing at a WIM station in Poland, Rys and Burnos (2021) observed that axle masses were concentrated near two peaks: the more frequent was around 11,500 kg, whereas the less frequent was near 4250 kg. Although they referred to just one single vehicle typology, the higher values observed for axle mass peaks (in our research) seem to indicate that there was more severe overloading at the Italian site than at the Polish site. More specifically, whereas the first peak relates to axles that comply with the maximum mass limit per axle imposed by the Italian Vehicle Code (12,000 kg), the second peak corresponds (at least partially) to axles that violate the mass limit regulations. A similar bimodal shape with a high peak at 1.4 m and a lower peak around 3.8 m was showed by the axle distance PDF. This finding can be explained by considering that common lorry configurations usually present with axle couples or triplets, which are closer to each other, interposed with longer void spaces (FHWA, 2022).

On the other hand, the speed parameter had a monomodal shape with a single peak at 66 km/h. Given that it is commonly known that vehicle speed tends to be normally distributed, this was an expected outcome (Martinelli et al., 2022a, Martinelli et al., 2022b). Similarly, the width parameter had a monomodal shape and was evenly distributed around 2.4 m, suggesting that this feature has a low variability amongst different vehicle groupings, probably due to the constraint imposed by the standardized dimensions of the roadway lanes.

Regarding discrete parameters, the PMF associated to axle number showed that the most prevalent typology for heavy lorries (representing roughly 88% of the total) was a five-axle configuration, followed by an eight-axle layout (representing approximately 7% of the total). The former is an expected result. Indeed, whilst previous literature showed that a six-axle configuration is the most common among freight lorries in China (Huang et al., 2022; Li et al., 2020), in Western countries a five-axle arrangement tends to prevail (Peng et al., 2021; Hernandez and Hyun, 2020; Micu et al., 2018; Fiorillo and Ghosn, 2018). As for categorical parameters, the CD related to axle typology indicated that single wheel axles made up around 64% of all the axle types, whilst double wheel axles were also relatively popular, accounting for about 36% of the total.

4.3. Adjusting the observed GVM to account for dynamic amplification phenomena

Next, according to Step 4, the DLF associated with each of the 14,861 passing vehicles was initially estimated by considering the response of a simply supported prismatic beam subjected to a constant force traveling at a constant speed, as indicated in Eq. (4). The PDF computed on the DLF (Fig. 4) showed a mean value of approximately 1.08, implying that the dynamic amplification phenomena were expected to increase the static GVM by about 8% for the case-study bridge.

Consequently, the "Dynamic" GVM of each passing vehicle was obtained by multiplying the static GVM by the DLF according to Eq. (5). Then the PDF computed on *dyn_GVM* (Fig. 5) showed a shape that resembles that which was associated with the *GVM* even though a) it was, as expected, shifted to the right due to dynamic amplification; b) it was more widely distributed (i.e., a lower maximum density was observed) due to the greater variability introduced by the existence of different passing speeds among the vehicles observed.

4.4. Fitting an MLR to predict the "Dynamic" GVM

According to Step 5, the explanatory factors were firstly computed on the parameters collected by the WIM system for each vehicle passing on the case-study bridge. Table 2 (which is self-explanatory) provides the list of these factors, their description, and some descriptive statistics.

A correlation matrix was determined to reveal if correlations between the explanatory factors exist. The results are shown in Table 3, which lists values and signs of correlation indexes between a pair-comparison of all factors.

The correlation indexes whose absolute value is greater than 0.8 are in bold font. It is worth noting that most of the correlation indexes among explanatory factors have rather small values, thus, potential multi-collinearity problems appear to be low. However, for some of the

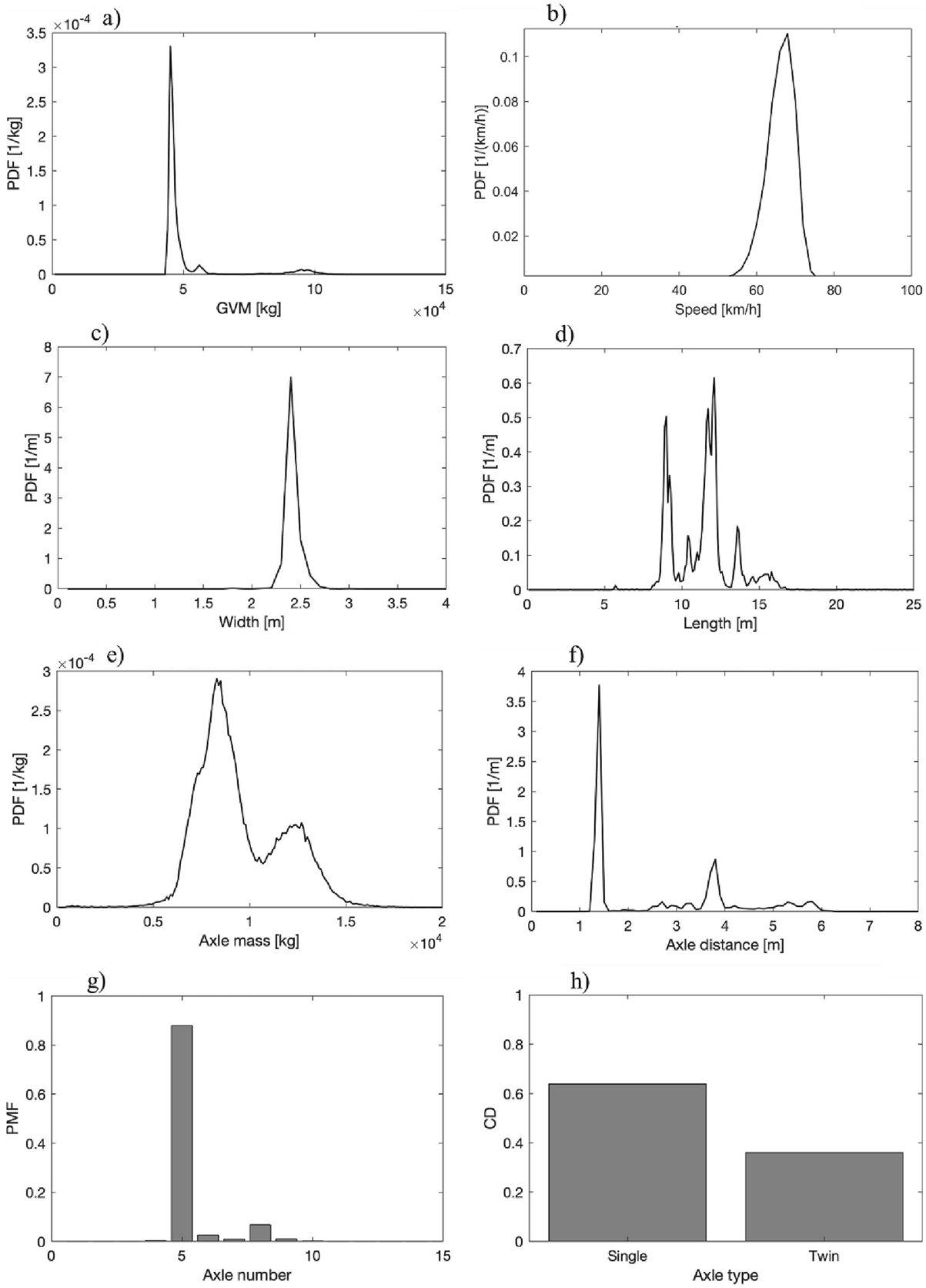

Fig. 3. A) PDF for GVM parameter b) PDF for speed parameter; c) PDF for width parameter; d) PDF for length parameter; e) PDF for axle mass parameter; f) PDF for axle distance parameter; g) PMF for axle number parameter; h) CD for axle type parameter. an earlier version of these images was reported in Ventura et al. (2023).

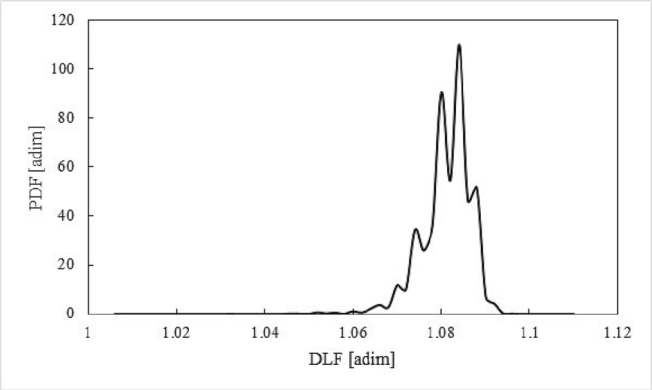

Fig. 4. PDF for the estimated DLF considering the response of a simply supported prismatic beam with travel at a constant speed.

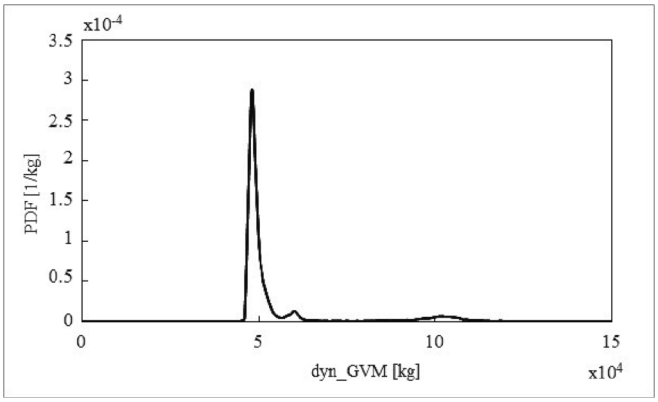

Fig. 5. PDF for the "Dynamic" GVM parameter.

12×12 pairs of explanatory variables, the pair-wise correlation indexes have values greater than 0.8, and, therefore, deserve some attention, since multi-collinearity issues could occur. Specifically, a strong positive correlation was found between the pairs (*max_int*; *std_int*), (*mean_int*; *std_int*) and (*mean_int*; *max_int*). Hence, two of the aforementioned explanatory factors (i.e., *max_int* and *std_int*) were eliminated based on the lowest correlations with the response variable. Moreover, a perfect negative correlation was found between the pair (*sing*; *doub*). Consequently, one of the two explanatory factors (i.e., *sing*) was removed by the database.

Next, a MLR model was built according to Eq. (6) to predict the "Dynamic" GVM of each vehicle as a function of explanatory factors (Table 2) that could be simply inferred without employing WIM devices. Table 4 provides the results of this best-fit model. In the upper part of the table, the coefficients estimated and their significances (p-value), which are in bold when <0.001, are indicated for each explanatory parameter included in the model. Finally, summary statistics and measures of errors are listed in the lower portion of Table 4.

Generally speaking, the MLR model accurately fits the experimental data. Indeed, it explains 91.9% of the "Dynamic" GVM variance, as indicated by R^2_{adj}. As for the F-test, the results indicate that the fitted MLR model has a high significance (p-value <0.001). Consequently, the null hypothesis that all regression coefficients are zero can be rejected. Furthermore, all the predictors were shown to be very significant (p-value <0.001), suggesting a strong regression effect. By establishing a 95% confidence interval, this finding is further supported. In fact, no generic null regression coefficient belongs to the stated interval (i.e., the null value is not comprised between the columns "Lower 95%" and "Upper 95%"). Consequently, this outcome endorses the assumption that an insignificant partial derivative can be rejected for each predictor amongst those included in the best fit MLR.

Focusing on the physical meaning and the coefficient sign of each predictor separately, the results indicate that five explanatory factors are positively correlated with the "Dynamic" GVM. This means that the "Dynamic" GVM increases as these factors increase as well whilst keeping all other factors constant at their means. More precisely:

- A 1 km/h increase in the passing speed leads to a 63.33 kg increase in the predicted "Dynamic" GVM. This was an expected outcome, since the dynamic amplification phenomena increase with the speed according to the DLF prediction model introduced in Step 4.
- A unit increase in the total axle number leads to a 27,843.81 kg increase in the predicted "Dynamic" GVM. This result is consistent as each axle has a fixed maximum load bearing capacity. Hence, more axles are needed to carry more mass.
- A 1% increase in the double wheel axle fraction leads to an approximately 82.55 kg increase in the predicted "Dynamic" GVM. This outcome was also expected because the double wheel axles can carry vehicle load in a more efficient way than single wheel axles due the greater contact area between the tyres and the road surface.
- A 1 m increase in mean axle distance leads to a 26,958.23 kg increase in the predicted "Dynamic" GVM. This consistent finding can be explained by the need to space out the heavier axles to reduce the load concentration on the structures.
- A 1 m increase in minimum axle distance leads to a 28,163.58 kg increase in the predicted "Dynamic" GVM. This consistent finding can be explained in the same manner as in the point above, i.e., by

Table 2
Explanatory factors computed on the parameters collected by the WIM system for each of the 14,861 vehicles passing on the case-study bridge during the two-month observation period. List, description, and some descriptive statistics.

Factor	Symbol	Unit	Type	Description	Mean	Std. Dev.	Min.	Max.
Day of the week	*Day*	–	Categorical	The day of the week when the vehicle was recorded	3.93	1.45	1.00	7.00
Time of day	*Hour*	–	Categorical	The time of day when the vehicle was recorded	10.37	4.42	0.00	23.00
Speed	*v*	*km/h*	Continuous	Mean passing speed among all vehicle axles	65.32	4.60	6.00	86.00
Width	*w*	*m*	Continuous	Mean width among all vehicle axles	2.37	0.07	1.49	3.02
Length	*l*	*m*	Continuous	Distance from the first and the last axle	11.34	1.95	1.92	35.12
Axle number	*axl*	*axles*	Discrete	Total number of vehicle axles	5.30	0.90	2.00	10.00
Single wheel axle fraction	*sing*	–	Discrete	Ratio between the number of vehicle axles with single wheels and the total number of axles	0.66	0.24	0.00	1.00
Double wheel axle fraction	*doub*	–	Discrete	Ratio between the number of vehicle axles with double wheels and the total number of axles	0.34	0.24	0.00	1.00
Mean axle distance	*mea_int*	*m*	Continuous	Mean of the vehicle axle distances	2.68	0.45	1.39	4.39
Std. dev. axle distance	*std_int*	*m*	Continuous	Standard deviation of the vehicle axle distances	1.63	0.45	0.00	3.98
Min axle distance	*min_int*	*m*	Continuous	Minimum of the vehicle axle distances	1.31	0.04	0.95	1.92
Max axle distance	*max_int*	*m*	Continuous	Maximum of the vehicle axle distances	4.68	0.95	1.39	10.96

Table 3
Correlation matrix for the explanatory factors and for the response variable. The correlation indexes whose absolute value is greater than 0.8 are in bold font.

	Day	*Hour*	*v*	*w*	*l*	*axl*	*sing*	*doub*	*mea_int*	*std_int*	*min_int*	*max_int*	*dyn_GVM*
Day	1.00												
Hour	−0.06	1.00											
v	−0.02	−0.01	1.00										
w	0.02	0.03	−0.03	1.00									
l	0.01	0.00	−0.04	−0.05	1.00								
axl	0.05	−0.04	−0.19	0.22	0.49	1.00							
sing	−0.03	0.04	0.13	−0.73	−0.12	−0.45	1.00						
doub	0.03	−0.04	−0.13	0.73	0.12	0.45	−1.00	1.00					
mea_int	−0.04	0.04	0.15	−0.26	0.54	−0.45	0.30	−0.30	1.00				
std_int	−0.04	0.07	0.15	−0.34	0.43	−0.39	0.44	−0.44	**0.84**	1.00			
min_int	0.01	−0.03	−0.08	0.33	0.18	0.16	−0.35	0.35	0.03	−0.21	1.00		
max_int	−0.03	0.07	0.12	−0.32	0.56	−0.26	0.37	−0.37	**0.83**	**0.98**	−0.14	1.00	
dyn_GVM	0.05	−0.05	−0.17	0.31	0.33	**0.93**	−0.53	0.53	−0.53	−0.48	0.24	−0.37	1.00

Table 4
Results associated to the MLR model that best fits the experimental data.

Explanatory factor (f)	Symbol	Coeff. Estimate (α_f)	p-value	Lower 95%	Upper 95%
Intercept	-	−103,057.24	**<0.001**	−108,237.01	−97,877.47
Speed	*v*	63.33	**<0.001**	46.08	80.59
Width	*w*	−8960.88	**<0.001**	−10,530.68	−7391.09
Length	*l*	−7518.13	**<0.001**	−7784.71	−7251.55
Total axle number	*axl*	27,843.81	**<0.001**	27,297.99	28,389.64
Double wheel axle fraction	*doub*	8255.32	**<0.001**	7730.58	8780.05
Mean axle distance	*mea_int*	26,958.23	**<0.001**	25,819.79	28,096.66
Min axle distance	*max_int*	28,163.58	**<0.001**	25,810.42	30,516.75

Summary statistics	**Value**
Adjusted R-squared	0.919
F value for overall significance	16772.00
p-value for overall significance	**<0.001**

Measures of errors	**Value (Training)**	**Value (Test)**	
Number of observations	10,403	4458	
MAE	2472.70	2538.20	[kg]
RMSE	4072.12	4172.44	[kg]
MAPE	0.0420	0.0434	
CoV	0.0752	0.0772	

the need to space out the heavier axles to reduce the load concentration on the structures.

Conversely, two explanatory factors are negatively correlated with the "Dynamic" GVM, which means that the "Dynamic" GVM decreases as these factors increase, whilst keeping all other factors constant at their means. More precisely:

- A 1 m increase in the vehicle width leads to an 8960.88 kg decrease in the predicted "Dynamic" GVM.
- A 1 m increase in the vehicle length leads to a 7518.13 kg decrease in the predicted "Dynamic" GVM.

These latter results are novel, and they contrast with the findings by Micu et al. (2018). Indeed, they found that larger vehicles had a greater probability to be heavier than shorter ones. However, there are at least three reasons that might explain these contrasting results. First, Micu et al. (2018) fitted their model on a sample composed by all vehicle typologies, including cars and light trucks. In a such wide set of observations, the greater variability of GVM and size parameters leads to a clear result with a positive relationship amongst the variables.

Conversely, in this case study, only extra-heavy lorries were considered when fitting the MLR model. Hence, in such a subsample, the existence of a positive correlation among GVM and size parameters would not be obvious. Second, the numerous iron and steel businesses that are active in the Brescia metropolitan area produce commodities that are heavy but not voluminous, due to the high density of metal materials. Consequently, haulers need not employ larger sized vehicles since such dense goods can be shipped using a more limited space. Third, the marble extracted in the quarries near the city is transported in smaller trucks as required by the reduced manoeuvring spaces available in the quarries. The latter two behaviours might raise safety questions that merit further research.

After analysing how predictors affect GVM, some statistics are provided to further assess the estimated model's performance. More precisely, the analysis of residuals and the prediction capacity of the MLR model are discussed in what follows. By applying Eqs. (7) and (8) to the residual analysis, a mean value of approximately 8.7963e-11 kg was obtained, which is effectively close to zero if compared with the order of magnitude of the GVM parameter. Actually, 94.6% of the residuals were no further than two standard deviations from the mean value, i.e., they were within the interval $\mu \pm 2\sigma$ ($\pm$8144.6 kg). This percentage was close to what would be expected if the residuals had a perfectly normal distribution, i.e., 95.45%. Moreover, Fig. 6 shows that the PDF of the residuals sufficiently overlaps the normal distribution. Therefore, although a greater concentration around the null value was observed for the PDF of the residuals if compared with the normal distribution, the former can be regarded as an acceptable fit of the latter.

As for the predicted performance of the model, the MoEs were computed according to Eqs. (9) to (12). The outcomes indicated that the fitted MLR had a good capacity for prediction. Indeed, when compared to the mean value of the predicted "Dynamic" GVM (i.e., 54,365 kg), the

MAE values for the training and test datasets (i.e., approximately 2473 kg and 2538 kg, respectively) can be regarded as worthy findings, as confirmed by the MAPE, which is lower than 4.5%. Moreover, the RMSE values for the training and test datasets (i.e., approximately 4072 kg and 4172 kg, respectively) can be considered as positive results, as confirmed by the CoV, which is lower than 8%. Particularly, the relatively low errors on the test dataset are a relevant result because this dataset has no effect on training and so provides an independent validation of the prediction accuracy of the proposed MLR.

Besides, it is worth noting that some could argue that assuming a linear relationship between the "Dynamic" GVM and explanatory factors could appear to be an oversimplification as opposed to other more refined formulations. To check if the linear model was not appropriated, additional different data fitting nonlinear models were considered, namely: logarithmic, exponential, power, and polynomial data.[1] As for the logarithmic, exponential, and power models, the fitting procedure repeatedly failed to converge to a solution, indicating that such functions were not a suitable fit for the case-study dataset.

Conversely, when considering polynomial models, a second order function showed that they had the best fit performance and slightly outperformed the linear model (the adjusted $R^2 = 0.946$ instead of 0.919). Nevertheless, despite the slightly greater performance of the second order polynomial model, the linear model was found to be preferable for the two reasons. First, the parsimony principle suggests that a simpler model with fewer parameters should be favoured over more complex models with more parameters, provided that the models fit the data well in a similar manner. Consequently, a trade-off between the goodness of a fitted model and the number of terms that needed to be evaluated to make "Dynamic" GVM predictions was pursued. Second, whilst the physical meaning of the coefficients associated with the linear model was straightforward, the coefficients associated to the second order polynomial model were more difficult to read, interpret and communicate, especially when interaction terms were subjected to focus. Truly, interaction terms would be difficult to manage if many variables were interacting with one another. Consequently, there was a trade-off between some predictive power and better comprehension of the coefficient's meanings, which would facilitate the understanding of the effect of the explanatory factors on "Dynamic" GVM predictions.

Finally, someone could point out that the established MLR model for predicting GVM is too simple compared with multi-source data fusion methods. However, data fusion methods are conceived for achieve a different goal than the MLR model proposed in this research, namely, accuracy the former, and cost-effectiveness the latter. Indeed, on the one hand, data fusion methods are aimed at reducing the uncertainty of WIM measurements by merging signals from many sensors (Gajda et al., 2020). Consequently, to implement these methods, large expenses need to be faced by RAs, because a great number of sensors need to be installed near the monitored bridge (Sroka et al., 2015). On the other hand, the MLR model proposed in this research is aimed at providing RAs with a straightforward (and cost-effective) tool to make a preliminary estimation of the GVM of the vehicles passing on bridges and thus aiding management actions. Consequently, the relatively lower accuracy of GVM predictions is traded with a less resource consuming estimation procedure.

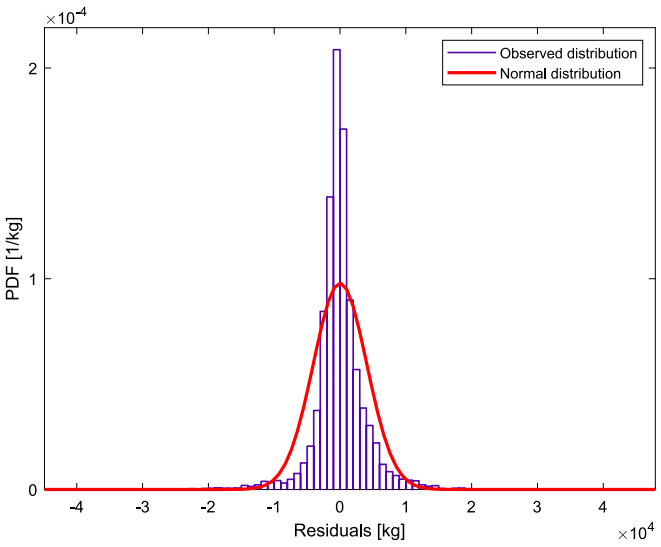

Fig. 6. Comparison between the observed distribution of the residuals and the normal distribution.

[1] Comparison among different typologies of models for predicting the "Dynamic" GVM. The acronym na indicates that the parameter is not available since the fitting procedure repeatedly failed to converge to a solution.

Item	Linear	Logarithmic	Exponential	Power	Polynomial (2nd order)
Number of coefficients	8	NA	NA	NA	36
Adjusted R-squared	0.919	NA	NA	NA	0.946
F value for overall significance	16,772	NA	NA	NA	78,780
p-value for overall significance	<0.001	NA	NA	NA	<0.001
MAE (Training)	2,472.70	NA	NA	NA	1,949.98
MAE (Test)	2,538.20	NA	NA	NA	2,060.40
RMSE (Training)	4,072.12	NA	NA	NA	3,294.25
RMSE (Test)	4,172.44	NA	NA	NA	4,020.77
MAPE (Training)	0.0420	NA	NA	NA	0.0336
MAPE (Test)	0.0434	NA	NA	NA	0.0340
CoV (Training)	0.0752	NA	NA	NA	0.0609
CoV (Test)	0.0772	NA	NA	NA	0.0742

5. Conclusions

The validity of polices aimed at preventing the structural damage caused by vehicles with permits and that are illegally overweight can be sustained by the adoption of WIM systems, which automatically and dynamically collect data on vehicle mass. Nevertheless, the relatively high installation and maintenance costs frequently prevent RAs from a widespread operational use of WIM systems. Indeed, whilst WIM devices and their use have been frequently studied and adopted in America and China, there have been fewer experiences in the field with these devices in Europe, most notably in Italy. Moreover, the link between gross vehicle mass (GVM) and other vehicle parameters has only been examined in earlier research in a fragmentary and qualitative manner. By processing and discussing real-world raw WIM data on 14,800+ overweight vehicles passing over an Italian case-study bridge, this paper has provided both theoretical and practical contributions to the research in two ways.

First, this case study refined the probability function distributions of several vehicular parameters to provide a broader insight of the main characteristics of passing vehicles. On the one hand, consistently with the findings of previous research, multimodal shapes were observed for the probability distributions of several parameters, suggesting the existence of several groups of vehicles of different typologies, including permits and illegally overloaded ones. On the other hand, the results suggested a more severe axle overloading phenomenon for the Italian site than those observed by other European authors.

Second, this study specified, calibrated, and validated a Multiple Linear Regression (MLR) model to provide RAs with a cost-effective tool to forecast the GVM of each overweight vehicle passing on bridges as a function of several vehicular predictors, without the need to install WIM systems along each road segment with bridges. Moreover, the effects of significant predictors on GVM were also investigated. Specifically, single- and double-wheel axles, along with mean and minimum axle distances, were the parameters that had the greater positive effects on the GVM predicted value. Conversely, the response variable showed a slight decrease as the length and width of the vehicle increased, whilst the MLR model achieved high predictive performance because the measurement of errors was low. To the best of our knowledge, this is the first time that raw WIM data has been explored to build a prediction model, in an Italian case study.

This case study has relevant implications because it provides practitioners, RAs, and governments with a) data related to vehicles with permits and those that are illegally overweight in a heavily industrialized Italian context, and b) a simple tool that can support management strategies for heavy vehicle traffic. Specifically, because WIM devices tend to be expensive to install near each bridge, RAs can manage the 'heavy' traffic (which may negatively affect the 'structural health') by using the MLR model to achieve a quick estimate of vehicle loads. As a result, the MLR prediction model might easily be implemented as a as a component of a less expensive monitoring system that can recognize traffic with large loads. Moreover, RAs could apply this model to identify those bridges where vehicles with permits and that are illegally overweight more severely exceed TC limits, which would enable certain management actions to be planned.

For example, traffic cameras with image processing algorithms might be used by RAs to collect the predictors needed by the MLR. These devices are less expensive than WIM devices, and they could be placed close in a denser way on their road network (also near bridges along secondary routes, where the high WIM investment expenses could appear to be not justified). As a result, RAs might straightforwardly forecast the "Dynamic" GVM of the vehicles with permits or that are illegally overweight before they cross the monitored bridges by executing the MLR model. Therefore, traffic management strategies could be implemented on the bridges where it is anticipated that heavier vehicles will travel. By using additional technology (e.g., traffic lights and variable message signals), these operations might reroute vehicles of which "Dynamic" GVM exceeds the bridge's carrying capacity by imposing them to quit the road at an exit upstream of the bridge.

Finally, this study indicates several developments. First, the MLR model could easily be enhanced by considering the likelihood of a vehicle being unloaded, partially loaded, or fully loaded, thus enhancing the GVM's predictive performance. Second, a new method could be developed for evaluating and managing the risks caused by traffic loads acting on bridges based on an ITS architecture, in real-time. This could be pursued through the probabilistic modelling of the frequency and severity of failure events calibrated to trigger signals aimed at avoiding the presence of an excessive vehicle load on bridges. Finally, though we only adopted traffic and weight variables collected by WIMs for this case study, the integration of new variables from other data acquired by different sensors (e.g., accelerometers, strain gauges, intelligent traffic cameras) should also be investigated to develop new predictive GVM models based on variables computed through the integration of multi-source data fusion algorithms.

CRediT authorship contribution statement

Roberto Ventura: Conceptualization, Methodology, Data curation, Formal analysis, Writing original draft, Writing – review & editing, Visualisation. **Benedetto Barabino:** Conceptualization, Methodology, Supervision, Writing – review & editing, Visualisation, Funding acquisition. **David Vetturi:** Supervision, Writing – review & editing. **Giulio Maternini:** Supervision, Writing – review & editing, Funding acquisition.

Declaration of Competing Interest

The authors declare that they have no known competing financial interests or personal relationships that could have appeared to influence the work reported in this paper.

Acknowledgments

The Provincia di Brescia signed a Research Agreement with the University of Brescia for the monitoring of the bridges along its road network, and the WIM station that acquired the data analysed in this paper is a part of that agreement. Moreover, this research was partially funded by:

- Regione Lombardia, Call Hub Ricerca e Innovazione, within the project "MoSoRe@Unibs—Infrastrutture e servizi per la Mobilità Sostenibile e Resiliente", 2020–2022, CUP E81B19000840007.
- European Union (EU) and Italian Ministry for Universities and Research (MUR), National Recovery and Resilience Plan (NRRP), within the project "Sustainable Mobility Center (MOST)", 2022–2026, CUP D83C22000690001, Spoke N° 7, "CCAM, Connected networks and Smart Infrastructures".
- Polis-Lombardia and the Safety Directorate General of the Lombardy Region within the Agreement on road safety studies to support the Road Safety Regional Monitoring Centre of the Lombardy Region (CMRL), cod. 221313OSS.
- Department of Civil, Environment, Land and Architecture Engineering and Mathematics (DICATAM), University of Brescia University of Brescia, within the research grant, CUP: D73C22000770002.

References

ARPA Lombardia, 2023. Archivio dati idro-nivo-meteorologici.

ASTM, 2017. ASTM E1318-09. Standard Specification for Highway Weigh-In-Motion (WIM) Systems with User Requirements and Test Methods.

Barabino, B., di Francesco, M., Mozzoni, S., 2017. Time reliability measures in bus transport services from the accurate use of automatic vehicle location raw data. Qual. Reliab. Eng. Int. 33 (5), 969–978. https://doi.org/10.1002/qre.2073.

Bosso, M., Vasconcelos, K.L., Ho, L.L., Bernucci, L.L.B., 2020. Use of regression trees to predict overweight trucks from historical weigh-in-motion data. J. Traffic Transp. Eng. (English Edition) 7 (6), 843–859. https://doi.org/10.1016/j.jtte.2018.07.004.

Cetin, M., Nichols, A.R., Chou, C.S., 2014. Reidentification of trucks on basis of axle-spacing measurements to facilitate analysis of weigh-in-motion accuracy. Transp. Res. Rec. 2443, 96–105. https://doi.org/10.3141/2443-11.

Chan, T.H.T., O'Connor, C., 1990. Vehicle model for highway bridge impact. J. Struct. Eng. (United States) 116 (7), 1772–1793. https://doi.org/10.1061/(ASCE)0733-9445(1990)116:7(1772).

Dan, D., Ying, Y., Ge, L., 2021. Digital twin system of bridges group based on machine vision fusion monitoring of bridge traffic load. *IEEE Trans. Intell. Transp. Syst.* https://doi.org/10.1109/TITS.2021.3130025.

De Aloe, M., Ventura, R., Bonera, M., Barabino, B., Maternini, G., 2023. Applying cost–benefit analysis to the economic evaluation of a tram-train system: evidence from Brescia (Italy). Res. Transp. Bus. Manag. 47, 100916 https://doi.org/10.1016/j.rtbm.2022.100916.

Demiroluk, S., Ozbay, K., Nassif, H., 2018. Mapping of truck traffic in New Jersey using weigh-in-motion data. IET Intel. Transport Syst. 12 (9), 1053–1061. https://doi.org/10.1049/iet-its.2018.0055.

Eurostat, 2022. Freight transport statistics - modal split. https://ec.europa.eu/eurostat/statistics-explained/index.php?title=Freight_transport_statistics_-_modal_split.

Faccin, C., Zavanella, L., Savoldi, E., Boroni, A., Rossini, P., 2011. Piano del traffico della viabilitá extraurbana (PTVE).

Fertlitsch, A., 2021. Deep Learning Patterns and Practices (Manning Publications, Ed.).

FHWA, 2022. Figure C-1 FHWA 13 Vehicle Category Classification. https://www.fhwa.dot.gov/policyinformation/tmguide/tmg_2013/images/figurec-1.jpg.

Fiorillo, G., Ghosn, M., 2018. Fragility analysis of bridges due to overweight traffic load. Struct. Infrastruct. Eng. 14 (5), 619–633. https://doi.org/10.1080/15732479.2017.1380675.

Fiorillo, G., Ghosn, M., 2019. Risk-based importance factors for bridge networks under highway traffic loads. Struct. Infrastruct. Eng. 15 (1), 113–126. https://doi.org/10.1080/15732479.2018.1496119.

Gajda, J., Sroka, R., Burnos, P., 2020. Sensor data fusion in multi-sensor weigh-in-motion systems. Sensors (Switzerland) 20 (12), 1–12. https://doi.org/10.3390/s20123357.
Ge, L., Dan, D., Yan, X., Zhang, K., 2020. Real time monitoring and evaluation of overturning risk of single-column-pier box-girder bridges based on identification of spatial distribution of moving loads. Eng. Struct. 210 (October 2019), 110383 https://doi.org/10.1016/j.engstruct.2020.110383.
Gungor, O.E., Al-Qadi, I.L., Mann, J., 2018. Detect and charge: Machine learning based fully data-driven framework for computing overweight vehicle fee for bridges. Autom. Constr. 96 (September), 200–210. https://doi.org/10.1016/j.autcon.2018.09.007.
Hernandez, S., Hyun, K., 2020. Fusion of weigh-in-motion and global positioning system data to estimate truck weight distributions at traffic count sites. J. Intell. Transp. Syst. Technol. Plann. Oper. 24 (2), 201–215. https://doi.org/10.1080/15472450.2019.1659793.
Hou, R., Jeong, S., Lynch, J.P., Law, K.H., 2020. Cyber-physical system architecture for automating the mapping of truck loads to bridge behavior using computer vision in connected highway corridors. Transp. Res. Part C: Emerging Technol. 111 (November 2019), 547–571. https://doi.org/10.1016/j.trc.2019.11.024.
Huang, P., Wang, J., Xu, X., Yang, G., Chen, S., Yuan, Y., Han, W., 2022. Improved multi-lane traffic flow simulation based on weigh-in-motion data. Measurement: J. Int. Measure. Confederation 188 (October 2021), 110408. https://doi.org/10.1016/j.measurement.2021.110408.
ISTAT, 2022. Popolazione Residente per età, sesso e stato civile al 1° gennaio 2022. https://demo.istat.it/popres/index.php?anno=2022&lingua=ita.
Italiana, R., 2015. Nuovo codice della Strada - D.Lgs. 285/1992 e s.m. Gazzetta Ufficiale Della Repubblica Italiana 115.
JSON.org, 2002. Introducing JSON. https://www.json.org/json-en.html.
Kim, J., Song, J., 2021. Bayesian updating methodology for probabilistic model of bridge traffic loads using in-service data of traffic environment. Struct. Infrastruct. Eng. 1–16. https://doi.org/10.1080/15732479.2021.1924797.
Iatsko, O., Nowak, A.S., 2021. Revisited Live Load for Simple-Span Bridges. J. Bridge Eng. 26 (1), 04020114. https://doi.org/10.1061/(asce)be.1943- 5592.0001647.
Lee, G.C., Mohan, S.B., Huang, C., Fard, B.N., 2013. A study of US bridge failures (1980–2012). MCEER Technical Rep. 1–148.
Li, M., Huang, T.L., Liao, J.J., Zhong, J., Zhong, J.W., 2020. WIM-based vehicle load models for urban highway bridge. Latin Am. J. Solids Struct. 17 (5), 1–20. https://doi.org/10.1590/1679-78255893.
Li, Q.J., Minnekanti, S.P., Yang, G., Wang, C., 2019. Traffic inputs for pavement ME design using Oklahoma data. Int. J. Pavement Res. Technol. 12 (2), 154–160. https://doi.org/10.1007/s42947-019-0020-5.
Liu, D., Deng, Z., Yinhai, W., Kaisar, E.I., 2020. Method for identifying truck traffic site clustering using weigh-in-motion (WIM) data. IEEE Access 8, 136750–136759. https://doi.org/10.1109/ACCESS.2020.3011433.
Liu, Y., Li, D., Li, Y., Zhang, Z., 2018. Estimation of extreme value vehicle load based on the extended Burr XII distribution. KSCE J. Civ. Eng. 22 (9), 3401–3408. https://doi.org/10.1007/s12205-017-1727-y.
Lu, N., Liu, Y., Beer, M., 2018. Extrapolation of extreme traffic load effects on a cable-stayed bridge based on weigh-in-motion measurements. Int. J. Reliab. Saf. 12 (1–2), 69–85. https://doi.org/10.1504/IJRS.2018.092504.
Ma, L., Zhang, W., Han, W.S., Liu, J.X., 2019. Determining the dynamic amplification factor of multi-span continuous box girder bridges in highways using vehicle-bridge interaction analyses. Eng. Struct. 181 (September 2017), 47–59. https://doi.org/10.1016/j.engstruct.2018.11.059.
Martinelli, V., Ventura, R., Bonera, M., Barabino, B., Maternini, G., 2022a. Effects of urban road environment on vehicular speed. Evidence from Brescia (Italy). Transp. Res. Procedia 60 (2021), 592–599. https://doi.org/10.1016/j.trpro.2021.12.076.
Martinelli, V., Ventura, R., Bonera, M., Barabino, B., Maternini, G., 2022b. Estimating operating speed for county roads' segments – Evidence from Italy. Int. J. Transp. Sci. Technol. https://doi.org/10.1016/j.ijtst.2022.05.007.
MathWorks, 2022a. jsondecode - Decode JSON-formatted *text*. https://it.mathworks.com/help/matlab/ref/jsondecode.html.
MathWorks, 2022b. struct - Structure array. https://it.mathworks.com/help/matlab/ref/struct.html.
Micu, E.A., Obrien, E.J., Malekjafarian, A., Quilligan, M., 2018. Estimation of extreme load effects on long-span bridges using traffic image data. Baltic J. Road Bridge Eng. 13 (4), 429–446. https://doi.org/10.7250/BJRBE.2018-13.427.
Micu, E.A., Malekjafarian, A., OBrien, E.J., Quilligan, M., McKinstray, R., Angus, E., Lydon, M., Catbas, F.N., 2019. Evaluation of the extreme traffic load effects on the Forth Road Bridge using image analysis of traffic data. Adv. Eng. Softw. 137, 102711.
Ministero delle Infrastrutture e dei Trasporti, 2020. Linee guida per la classificazione e gestione del rischio, la valutazione della sicurezza ed il monitoraggio dei ponti esistenti.
Mitoulis, S.A., Domaneschi, M., Cimellaro, G.P., Casas, J.R., 2021. Bridge and transport network resilience – a perspective. In: Proceedings of the Institution of Civil Engineers – Bridge Engineering, pp. 1–12. https://doi.org/10.1680/jbren.21.00055.
Moghimi, H., Ronagh, H.R., 2008. Impact factors for a composite steel bridge using non-linear dynamic simulation. Int. J. Impact Eng 35 (11), 1228–1243. https://doi.org/10.1016/j.ijimpeng.2007.07.003.
OIML, 2006. OIML R 134-1: Automatic instruments for weighing road vehicles in motion and measuring axle loads Part 1: Metrological and technical requirements – Tests. 2006, 1–81.
Peng, C., Jiang, Y., Li, S., Nantung, T., 2021. Neural network optimal model for classification of unclassified vehicles in weigh-in-motion traffic data. Transp. Res. Rec. 2675 (7), 11–23. https://doi.org/10.1177/0361198121990670.
Regehr, J.D., Maranchuk, K., Vanderwees, J., Hernandez, S., 2020. Gaussian mixture model to characterize payload distributions for predominant truck configurations and body types. J. Transp. Eng., Part B: Pavements 146 (2), 04020017. https://doi.org/10.1061/jpeodx.0000174.
Ren, J., Thompson, R.G., Zhang, L., 2019. Impact of payload spectra of heavy vehicles on pavement based on weigh-in-motion data. J. Transp. Eng., Part B: Pavements 145 (2), 04019005. https://doi.org/10.1061/jpeodx.0000099.
Rivera-Royero, D., Jaller, M., Kim, C.M., 2021. Spatio-temporal analysis of freight flows in southern california. Transp. Res. Rec. 2675 (9), 740–755. https://doi.org/10.1177/03611981211004130.
Rys, D., Burnos, P., 2021. Study on the accuracy of axle load spectra used for pavement design. Int. J. Pavement Eng. 1–10. https://doi.org/10.1080/10298436.2021.1915492.
Shrestha, N., 2020. Detecting multicollinearity in regression analysis. Am. J. Appl. Math. Stat. 8 (2), 39–42. https://doi.org/10.12691/ajams-8-2-1.
Sroka, R., Gajda, J., Burnos, P., Piwowar, P., 2015. June 24). Information fusion in weigh in motion systems. In: SAS 2015–2015 IEEE Sensors Applications Symposium. https://doi.org/10.1109/SAS.2015.7133637.
Sujon, M., Dai, F., 2021. Application of weigh-in-motion technologies for pavement and bridge response monitoring: State-of-the-art review. Automation in Construction 130 (July), 103844. https://doi.org/10.1016/j.autcon.2021.103844.
Ventura, R., Barabino, B., Vetturi, D., Maternini, G., 2020. Bridge safety analysis based on the function of exceptional vehicle transit speed. Open Transp. J. 14 (1), 222–236. https://doi.org/10.2174/1874447802014010222.
Ventura, R., Barabino, B., Vetturi, D., Maternini, G., 2023. Bridge's vehicular loads characterization through Weight-In-Motion (WIM) systems. The case study of Brescia. European Transport/Trasporti Europei, 00(90), 1–12. 10.48295/ET.2023.90.6.
Yang, G., Wang, P., Han, W., Chen, S., Zhang, S., Yuan, Y., 2021. Automatic generation of fine-grained traffic load spectrum via fusion of weigh-in-motion and vehicle spatial–temporal information. Comput. Aided Civ. Inf. Eng. 1–15 https://doi.org/10.1111/mice.12746.
Yannis, G., Antoniou, C., 2005. Integration of weigh-in-motion technologies in road infrastructure management. ITE J. (Institute of Transportation Engineers) 75 (1), 39–43.
Zanini, M.A., Faleschini, F., Pellegrino, C., 2017. Probabilistic seismic risk forecasting of aging bridge networks. Eng. Struct. 136, 219–232. https://doi.org/10.1016/j.engstruct.2017.01.029.
Zhang, G., Liu, Y., Liu, J., Lan, S., Yang, J., 2022. Causes and statistical characteristics of bridge failures: A review. J. Traffic Transp. Eng. (English Edition) 9 (3), 388–406. https://doi.org/10.1016/j.jtte.2021.12.003.
Zhao, J., Wang, H., Lu, P., 2021. Impact analysis of traffic loading on pavement performance using support vector regression model. Int. J. Pavement Eng. 1–13. https://doi.org/10.1080/10298436.2021.1915493.
Zhou, J., Caprani, C.C., Zhang, L., 2021. On the structural safety of long-span bridges under traffic loadings caused by maintenance works. Eng. Struct. 240 (February), 112407 https://doi.org/10.1016/j.engstruct.2021.112407.